# Conductive Black Silicon Surface Made by Silver Nanonetwork Assisted Etching

*Chuan Fei Guo, Tianyi Sun, Yang Wang, Jinwei Gao, Qian Liu,* Krzysztof Kempa,* and Zhifeng Ren**

Energy and environmental problems have raised great concerns in recent years. The conversion of sunlight to electricity is one of the promising ways to solve the energy and environmental problems. The most widely used devices for solar energy harvesting are single crystalline silicon (c-Si) solar cells, with a worldwide installed capacity of over 60 GW,[1] which can convert solar energy directly into electricity. The conversion efficiency of solar cells can be improved by boosting light trapping in the cell, and assuring a very high conductivity and transparency of the window electrodes. Several approaches have been developed for improving light trapping: making pyramidal surface textures or other micro-/nanostructures,[2–6] scattering light with metallic nanoparticles,[7–9] depositing an anti-reflection coating (ARC),[10] and fabricating plasmonic metallic structures,[11–16] and for improving electrode conductivity: metallic grids or conducting oxide films are often applied. For example, commercial c-Si solar cells often adopt a pyramidally textured Si surface covered by an ARC, displaying a high absorbance of ~95%; Ag finger electrodes by screen printing are used to get a good conductivity. Light absorbance often compromises electrical conductivity in commercial c-Si solar cells. On a large area device, a screen printed solar cell may have shading losses as high as 10 to 15%.

Dr. C. F. Guo, Prof. Q. Liu
National Center for Nanoscience and Technology
China, No. 11 Beiyitiao Zhongguancun
Beijing 100190, China
E-mail: liuq@nanoctr.cn

Dr. C. F. Guo, T. Sun, Prof. Z. Ren
Department of Physics and TcSUH
University of Houston
Houston, TX 77204, USA
E-mail: zren@uh.edu

T. Sun, Prof. K. Kempa
Department of Physics
Boston College, Chestnut Hill, MA 02467, USA
E-mail: kempa@bc.edu

Prof. Y. Wang, Prof. J. Gao
Institute for Advanced Materials
Academy of Advanced Optoelectronics
South China Normal University
Guangzhou 510006, China

DOI: 10.1002/smll.201300718

To solve this problem, some technologies were developed to minimize or even eliminate the shading losses of the metal electrodes. Back contact solar cells (e.g., emitter wrap-through solar cells) and buried contact solar cells were developed for this purpose.[17,18] However, these technologies often involve quite complicated processes and hence the cost is higher. Here we report a novel c-Si structure with buried silver nanonetwork (SNN), exhibiting both low reflectance (~3% in the range of 400–1000 nm, without ARC) and good surface electrical conductivity (with sheet resistance down to 6 Ω/□). The SNN is made by a nonlithographic nanofabrication process, and it goes into Si by a simple chemical catalytic etching, which creates low-reflected submicron Si islands surrounded with the SNN. This work may offer a new way toward ARC-free c-Si (or other semiconductors like GaAs) solar cells, for which the absorbance does not conflict with electrical conductivity.

The conductive black silicon surface (CBSS) with Si islands is made by a bilayer lift-off metallization technique. Here the bilayer consists of an In mask layer on a $SiO_x$ sacrificial layer for undercut formation. **Figure 1**(a) shows the route for the CBSS fabrication. We first deposited a 65 nm thick $SiO_x$ layer on a flat and clean silicon wafer, and subsequently a 100 nm thick indium (In) monolayer made of closely packed islands. These islands are typically several hundreds to one micron in diameter, and gaps between islands are quite small. An isotropic etching of the In film in 20 wt% $HNO_3$ can widen the gaps lineally with the increasing of etching time. The as-etched indium island film is then passivated by thermal oxidation at 400 °C for 1 h. After that the sample is rinsed in 5% HF for 15 s; the limited rinse time guarantees that only the $SiO_x$ near the gaps gets dissolved, leading to the formation of undercuts. The passivation of the In film is necessary because In is dissolvable in HF. And then 3 nm Ti and 40 nm Ag are subsequently deposited on the bilayer-capped wafers, which are finally rinsed in preblended solution of 0.6% $H_2O_2$ and 10% HF for catalytic etching.[19] The $In_2O_3$ grains are finally removed by either ultrasonication or uniform wiping with wet lens paper.

Figure 1(b) and (c) show SEM images of an In island monolayer on $SiO_x$, before and after $HNO_3$ etching. The latter reveals a gap network with a quite uniform width of tens of nanometers. Figure 1(d) and its inset are SEM images of the sample after undercut formation and metal deposition, showing that a metal nanomesh is formed in the gaps. And


© 2013 Wiley-VCH Verlag GmbH & Co. KGaA, Weinheim

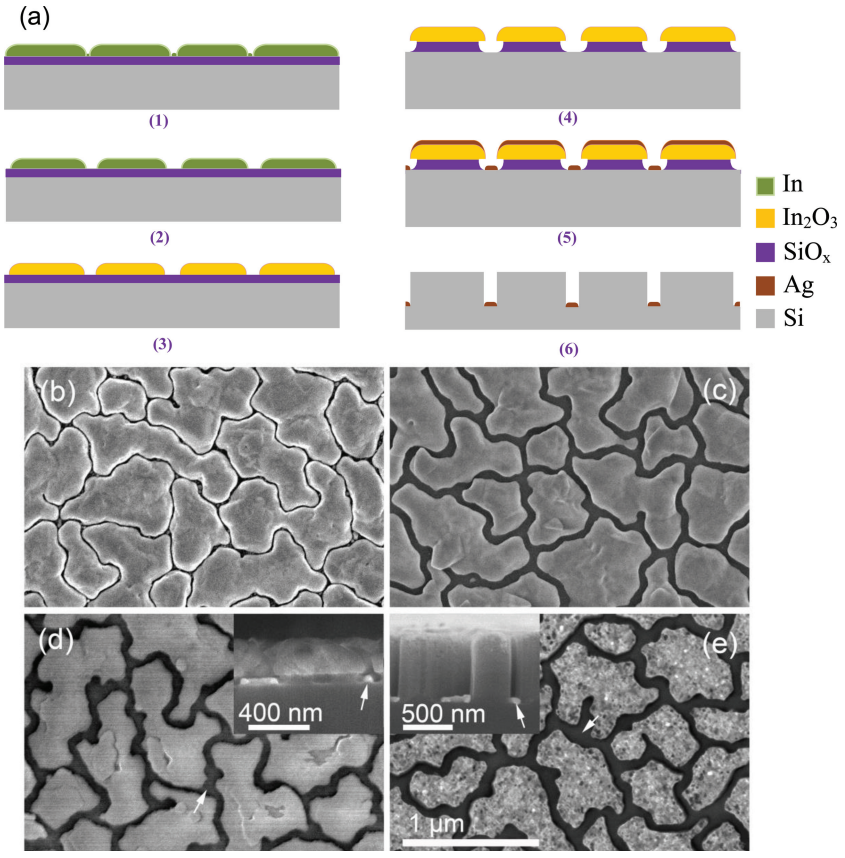


**Figure 1.** (a) Schematic illustration of the fabrication of CBSS. (1) Deposition of In/$SiO_x$ bilayer on a Si wafer. (2) Gap formation by etching in diluted $HNO_3$. (3) Passivation of In islands. (4) Undercut formation by rinsing in diluted HF. (5) Deposition of Ag film, leading to the formation of a Ag nanonetwork in the grooves. (6) Catalytic etching, during which the Ag nanonetwork digs into Si wafer and $In_2O_3$ grains get removed. (b)-(e) SEM images corresponding to steps (1), (2), (5) and (6). The arrows in panels (d) and (e) indicate the Ag nanonetwork.

Figure 1(e) is a CBSS with Si islands surrounded by a well-connected metal nanonetwork. The width and configuration of the metal nanonetwork are determined by the gaps which are formed with $HNO_3$ etching. To our best knowledge, this is the first report on nanofabrication by etching well-connected grain boundaries as the template for metallization, and the nanowire width can be controlled from tens of to more than 100 nm.

The CBSS samples are black, indicating good light absorption. We measured reflectance spectra of the samples both with and without ARC by an integrating sphere spectrometer (Ocean Optics, USB4000 VIS-NIR-ES). **Figure 2**(a) shows reflectance spectra of a sample with a silicon island size (or average Ag network mesh size) of 650 nm, Ag network depth of 600 nm and wire-width of 80 nm, before and after ARC deposition. In the wavelength range of 400–1000 nm, the samples with and without ARC demonstrate average solar reflectance 2.0 and 3.2%, respectively. In addition, reflectance of three other samples: bare Si wafer, Ag network on flat Si, and Ag network on crest of inverted Si pyramids, are also shown for comparison. The Ag network on Si wafer reveals a reflectance of ~40%, which is ~8% higher than that of a bare Si wafer. And the sample with Ag network on crest of textures reveals a reflectance of ~10%. These results indicate that Ag network on a flat surface or the top of textures (like inverted pyramids) is relatively reflective; in comparison, the buried Ag network does not significantly affect the reflectance. For the CBSS, light gets scattered by the grooves and absorbed in Si. As the grooves templated by the SNN are less than 100 nm wide, much smaller than the light wavelength, light cannot directly get into the grooves and hit the silver network. Therefore, the buried metal electrode should be a good structure for low reflectance Si surface. We also find that depth of SNN can dramatically influence the reflectance of the samples. Silicon wafers with Ag network on the flat surface (depth = 0) have a high reflectance of ~40%. But when the Ag nanonetwork depth increases to 200 nm or more, we could get a low reflectance of smaller than 8.0% for samples without ARC, or smaller than 3.0% for samples with

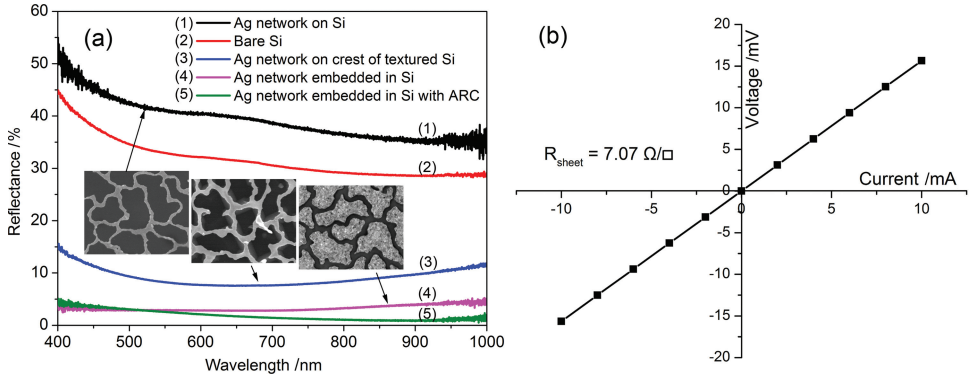


**Figure 2.** (a) Reflectance spectra of different samples: (1) Ag network on flat Si; (2) bare Si wafer; (3) Ag network on crest of pyramidally textured Si; (4) Ag network embedded in Si; and (5) Ag network embedded in Si (with ARC). Insets are SEM images of samples corresponding to (1), (3) and (4). (b) I-V characteristic of a CBSS sample with Ag nanowire width of ~80 nm and thickness of 40 nm.


© 2013 Wiley-VCH Verlag GmbH & Co. KGaA, Weinheim

small NANO MICRO

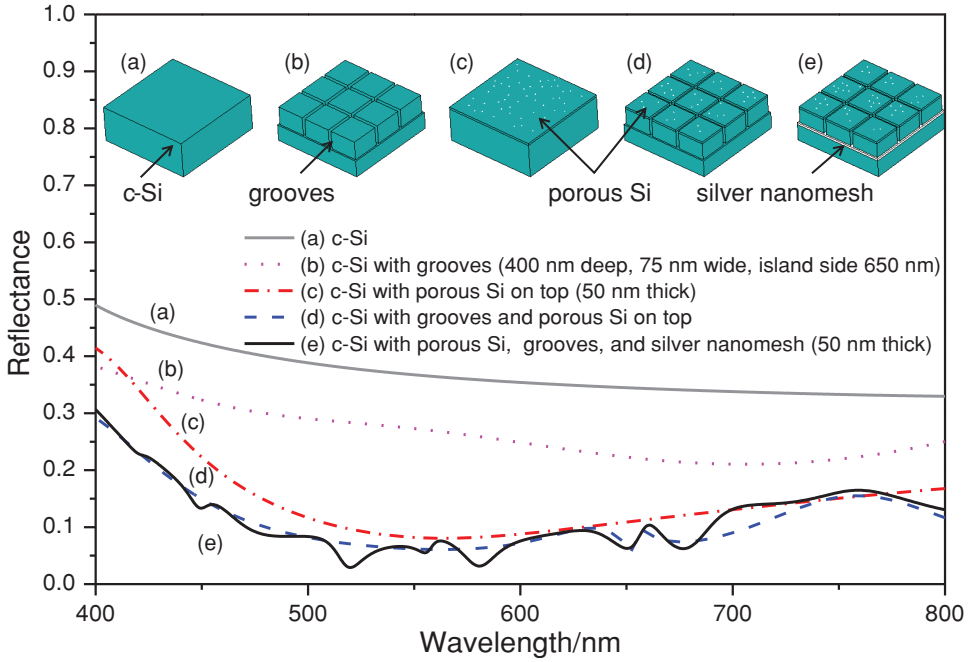


**Figure 3.** Reflectance of five different structures by FDFD simulation. (a) c-Si (grey solid line), (b) c-Si with grooves (dot line), (c) c-Si topped with porous silicon (Maxwell-Garnett model, 60% air volume fraction) (red dash dot line), (d) c-Si grooves and topped with porous Si (blue broken line), and (e) c-Si with porous Si, grooves, and Ag nanomesh (black solid line).

ARC. Further increase of the depth to more than 400 nm could not significantly decrease reflectance. Removal of the Ag network from CBSS does not cause a significant decrease of reflectance (~1%), implying that the Ag nanonetwork in the grooves does not obviously influence optical properties of the CBSS samples (Figure S1).

The measured reflectance of the samples is lower than most light-harvesting devices such as commercial silicon solar cells, implying that it may have potential applications in high efficiency light harvesting devices. Besides good light absorption, the CBSS also presents quite good surface electrical conductivity. For example, Figure 2(b) demonstrates that the sample with a 97% absorbance presents a sheet resistance of 7 Ω/□, which is much better than ITO films. The electrical conductivity can be further improved by decreasing mesh size, adding metal thickness and width.

The low reflectance of CBSS stems from two levels of surface microstructures. The first level is the obvious grooves and islands generated by the nanomesh assisted chemical etching, and the second level is the small porosity in each of the Si islands, formed by the catalytic etching with Ag fragments/nanoparticles (Figure 1(e)). It is a combined effect of the two levels of microstructures that reduces the reflectance to ~3%. In addition, plasmonic effects of the SNN and small Ag nanoparticles in the pores may also cause light trapping.[15] However, due to the fact that these Ag nanostructures are buried hundreds of nanometers deep, such effect should be very small.

Finite-difference-frequency-domain (FDFD) simulation (Computer Simulation Technology, Microwave Studio) is employed to capture the main physics of these microstructures (**Figure 3**). The Maxwell-Garnett model is applied to model the dielectric function of the porous surface.[20] Without grooves, the porous surface results in a reflectance of ~10%. This agrees with the experimental results for Si wafers with a similar surface (obtained by catalytic etching of a flat Si wafer with Ag nanoparticles on the surface, see Figure S2). When the grooves are added (modeled as a perfectly periodic mesh), the simulation shows that the reflectance decreases further to below 10%, and remains essentially unchanged when the silver nanomesh is placed into the grooves (CBSS structure), even though more than 20% of the surface area is shaded by the metal mesh. This is due to the deep embedding mechanism, which we have discussed. If there is no porous Si layer, then the reflectance will be much higher. These simulation results are at least in a qualitative agreement with the experiments. The slightly larger reflectance in the simulation is the result of the model assumptions. Firstly, the effective medium theory is strictly valid only in long wavelength limit, and thus a discrepancy between the simulation and experiment is expected on the short wavelength side of the visible range. Secondly, the irregularity of the island shapes and the aperiodicity is ignored. In the experiments, this irregularity contributes to light scattering within and between the grooves, leading to a reduced reflectance.

For most light-trapping structures, it is difficult to keep both high absorption and good electrical conductivity. Metallic electrodes are often used to achieve good electrical conductivity. But since metal is reflective, it compromises the light absorption. For example, in monocrystalline silicon solar cells, Ag finger electrodes are used to improve electrical conductivity, but those fingers also lead to a light


© 2013 Wiley-VCH Verlag GmbH & Co. KGaA, Weinheim

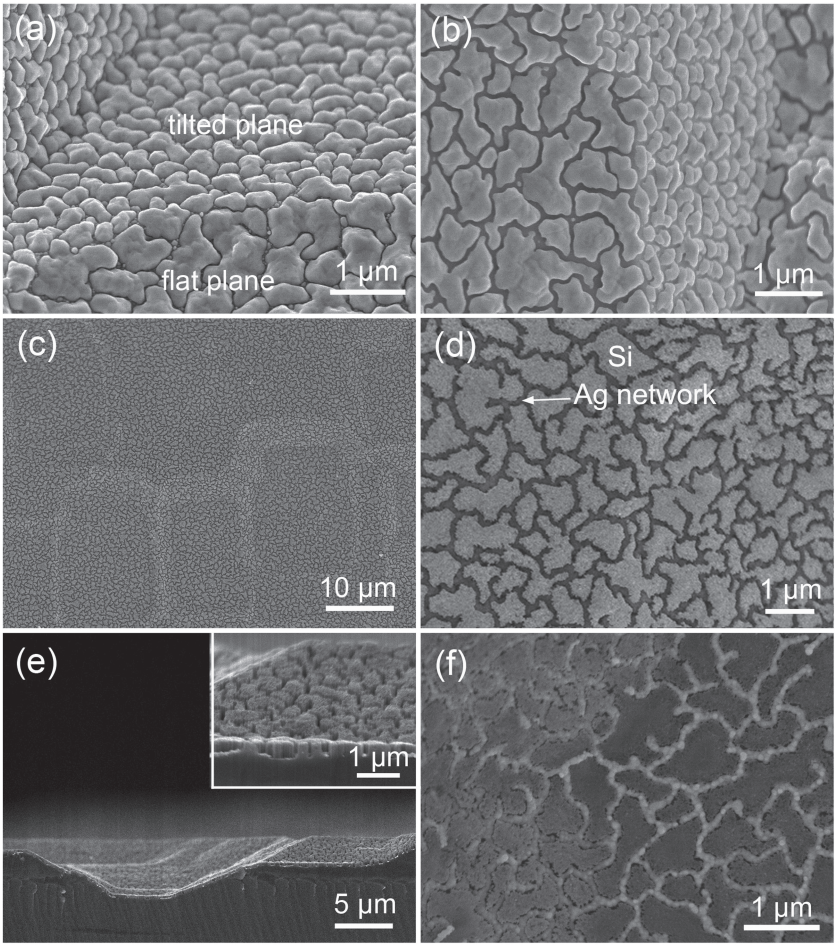


**Figure 4.** In/$SiO_x$ bilayer on a non-polished Si wafer before (a) and after (b) $HNO_3$ etching. (c) and (d) Low and medium magnification image of the CBSS, corresponding Ag nanonetwork depth is 400 nm. (e) Cross section SEM image of the SBSS corresponding to panel (d). (f) A sample with Ag network depth of 150 nm.

shading effect over the underlying silicon, resulting in a lower light absorption. However, our conductive black silicon surface (CBSS) presents both high electrical conductivity and good light absorbance, and the two are almost mutually independent. With a 45 nm thick Ag nanonetwork (wire-width ~90 nm), the CBSS can present a sheet resistance close to 6 Ω/□, while keep a high absorbance of larger than 95%. The absorbance can be further increased to 98% by depositing an ARC. Although the Ag network shades 20~30% of the silicon, it does not proportionally increase reflectance because the network is buried several hundred nanometers deep from the silicon surface (Figure 3). Even when the Ag network is removed from the grooves, the reflectance only has a small decrease of ~1%. Of course, some of the light energy is absorbed by the silver network. This, however, is a small effect, even in the ultra-thin absorber cells.[21,22]

In order to show that the technique can be applied to other cases, we have also successfully made such structures on non-polished Si wafers. Here the non-polished Si surface is made up of many crystallographically flat planes. **Figure 4**(a) and (b) show In grain films on a $SiO_x$/Si structure, before and after etching in $HNO_3$, respectively. The only difference between In grains on horizontal planes and those on tilted planes is that the ones in the latter are smaller. And we notice that since the gaps of the tilted planes are partially shaded by the In grains, we have to use magnetron sputtering, which can deposit Ag into shaded gaps to make Ag networks. Figure 4(c) and (d) are SEM images of the CBSS (Ag network depth: 400 nm) taken at different magnifications, showing that Ag nanowires in both horizontal and tilted planes are well connected. Figure 4(e) is the corresponding cross section image, and we could see the surface of Si islands is porous. This sample presents a high absorption of 97.0%. Figure 4(f) is a sample with Ag network shallowly buried, with a depth 150 nm. Compared with the counterpart in Figure 4(e), surface of Si islands here is much smoother and the corresponding absorption is ~90%. This is evidence that long time catalytic etching results in a deeper Ag network and a more porous Si surface and hence leads to a higher absorption.

In conclusion, we have successfully developed a scalable and cost-effective way to fabricate Ag nanonetwork embedded in silicon to form conductive black silicon surface (CBSS), by using In/$SiO_x$ bilayer lift-off metallization and catalytic etching. $HNO_3$ etched In island film after oxidation serves as a mask for the follow-up deposition and etching. The CBSS possesses a high light absorption up to 97% (without ARC) and a low sheet resistance close to 6 Ω/□. Our simulation suggests that the high absorption stems from the two kinds of surface microstructures: the islands/grooves structure and the porous surface of the Si islands. The CBSS might find applications where high light absorption and high electrical conductivity are required simultaneously. However, carrier recombination at the Si/metal interface should be a further concern for the application of CBSS.

## Experimental Section

*Fabrication of Ag Nanonetworks and CBSSs*: The $SiO_x$ film (65 nm) and In films (100 nm) were deposited by using a magnetron sputter (AJA International Inc., ORION-8 magnetron sputtering system), and the Ag films were deposited by using an electron beam evaporation system (Sharon). The CBSSs were simply made by rinsing the Ag network in step (5) in blended solution of HF (10%) and $H_2O_2$ (0.6%) for 20–40 s under ultrasonication.

*Characterization*: Morphology of the samples was taken by using a JEOL 6340F scanning electron microscope. Reflectance spectrum was recorded with a spectrometer (Ocean Optics, USB4000 VIS-NIR-ES, ISP-REF) in the wavelength range from


© 2013 Wiley-VCH Verlag GmbH & Co. KGaA, Weinheim

NANO MICRO small

400 to 1000 nm. Sheet resistance was measured by using the van der Pawn method, with four electrodes at four corners of a square of the sample and recorded with a Keithley 2400 meter and an Agilent 34401A meter.

## Supporting Information

*Supporting Information is available from the Wiley Online Library or from the author.*

## Acknowledgements

*C. F. Guo and T. Sun contributed equally to this work. The work performed at University of Houston and Boston College is funded by the US Department of Energy under Contract Number DOE DE-FG02-00ER45805, the part performed at National Center for Nanosci. & Tech, is supported by the funds of NSFC (10974037), NBRPC (2010CB934102), International S&T Cooperation Program (2010DFA51970), and the work performed at South China Normal University is supported by Thousands of Talent Program (2010), the leading talents of Guangdong Province (2010 and 2011), and NSFC under Contract No. 61106061.*

[1] W. Weiss, F. Mauthner, *International Energy Agency* **2010**, www.iea-shc.org.
[2] P. Campbell, M. A. Green, *J. Appl. Phys.* **1987**, *62*, 243.
[3] J. Zhao, A. Wang, M. A. Green, *Appl. Phys. Lett.* **1998**, *73*, 1991.
[4] Y. Liu, T. Lai, H. Li, Y. Wang, Z. Mei, H. Liang, Z. Li, F. Zhang, W. Wang, A. Y. Kuznetsov, X. Du, *Small* **2012**, *8*, 1392.
[5] B. Wang, P. W. Leu, *Nanotechnology* **2012**, *23*, 194003.
[6] H. Jin, G. L. Liu, *Nanotechnology* **2012**, *23*, 125202.
[7] F. J. Beck, A. Polman, K. R. Catchpole, *J. Appl. Phys.* **2009**, *105*, 114310.
[8] Y. Zhang, Z. Ouyang, N. Stokes, B. Jia, Z. Shi, M. Gu, *Appl. Phys. Lett.* **2012**, *100*, 151101.
[9] K. R. Catchpole, A. Polman, *Appl. Phys. Lett.* **2008**, *93*, 191113.
[10] J. Müller, B. Rech, J. Springer, M. Vanecek, *Solar Energy* **2004**, *77*, 917.
[11] V. E. Ferry, L. A. Sweatlock, D. Pacifici, H. A. Atwater, *Nano Lett.* **2008**, *8*, 4391.
[12] Z. Yu, A. Raman, S. Fan, *Opt. Express* **2010**, *18*, A366.
[13] H. A. Atwater, A. Polman, *Nat. Mater.* **2010**, *9*, 205.
[14] K. Aydin, V. E. Ferry, R. M. Briggs, H. A. Atwater, *Nat. Commun.* **2011**, *2*, 517.
[15] M. Seol, S. Choi, D. J. Baek, T. J. Park, J. Ahn, S. Y. Lee, Y. Choi, *Nanotechnology* **2012**, *23*, 095301.
[16] Y. Wang, E. W. Plummer, K. Kempa, *Adv. Phys.* **2011**, *60*, 799.
[17] J. M. Gee, W. K. Schubert, P. A. Basore, Photovoltaic Specialists Conference, 1993, Conference Record of the Twenty Third IEEE **1993**, 265.
[18] S. Narayanan, J. H. Wohlgemuth, J. B. Creager, S. P. Roncin, J. M. Perry, Photovoltaic Specialists Conference, 1993, Conference Record of the Twenty Third IEEE **1993**, 277.
[19] K.-Q. Peng, S.-T. Lee, *Adv. Mater.* **2011**, *23*, 198.
[20] J. C. M. Garnett, *Phil. Trans. R. Soc. Lond. A* **1906**, *205*, 237.
[21] Y. Wang, T. Sun, T. Paudel, Y. Zhang, Z. Ren, K. Kempa, *Nano Lett.* **2012**, *12*, 440.
[22] T. Sun, E. M. Akinoglu, C. Guo, T. Paudel, J. Gao, Y. Wang, M. Giersig, Z. Ren, K. Kempa, *Appl. Phys. Lett.* **2013**, *102*, 101114.

Received: March 7, 2013
Revised: April 21, 2013
Published online: June 13, 2013


© 2013 Wiley-VCH Verlag GmbH & Co. KGaA, Weinheim